Reconnecting the Fractured: Nanowire Networks and the Physics of Bridge Percolation

Amaury BARET

Department of Physics, SPIN, University of Liège, Allée du Six Août 19, B–4000 Liège, Belgium Correspondence to: abaret@uliege.be

Received: 19 April 2025 – Accepted 5 November 2025 This work is distributed under the Creative Commons CC BY 4.0 Licence.

Cet article a reçu le Prix Annuel 2025 de la Société Royale des Sciences de Liège. This paper was awarded the Annual Prize 2025 of the Société Royale des Sciences de Liège.

Abstract

As the demand for sustainable material solutions to address climate change intensifies, the development of energy-efficient materials has become a major focus of research. Transparent conducting materials play a central role in this effort, with silver nanowire networks emerging as promising candidates thanks to their flexibility and low material consumption. In this study, we introduce fundamental concepts from percolation theory to investigate the complex behavior of these intrinsically disordered, nanoscale systems. We then present the original concept of bridge percolation, a novel mechanism by which sparse nanowires restore conductivity across fractured thin films. Using high-performance computing, we validate a predictive, parameter-free model that captures this phenomenon and reveals the potential for ultra-low material use. This work offers both theoretical insight and practical pathways toward next-generation, sustainable transparent materials.

Keywords: bridge percolation, silver nanowire networks, transparent conducting materials

Résumé

Reconnecter ce qui est fracturé : les réseaux de nanofils et la physique de la bridge percola-

tion Face à l'urgence climatique, le développement de technologies énergétiquement efficaces suscite un intérêt croissant. Les matériaux transparents conducteurs jouent un rôle central dans cette transition, et les réseaux de nanofils d'argent s'imposent comme des candidats prometteurs grâce à leur flexibilité et à leur faible consommation de matériaux. Dans ce travail, nous introduisons les concepts fondamentaux associés à la théorie de la percolation afin d'explorer le comportement complexe de ces systèmes intrinsèquement désordonnés. Nous présentons ensuite le concept original de *bridge percolation*, un mécanisme permettant à des nanofils dispersés de rétablir la conductivité à travers des couches minces fracturées. À l'aide de calculs numériques haute performance, nous validons un modèle analytique prédictif sans paramètre

ajustable, révélant la possibilité d'une conduction efficace avec une quantité de matériau extrêmement réduite. Ce travail, à la croisée des mathématiques et de la science des matériaux, ouvre des perspectives théoriques et technologiques vers une nouvelle génération de matériaux transparents conducteurs durables.

Mots-clés : bridge percolation, réseaux de nanofils d'argent, matériaux transparents conducteurs

1. Introduction

A fundamental aspect of human civilization is its reliance on solid materials. The ability to manipulate and innovate with materials has been a driving force behind technological, economic, and societal transformations. Throughout history, breakthroughs in material science have marked major paradigm shifts, as reflected in the names of famous historical periods: the Stone Age, the Bronze Age, the Iron Age, and, more recently, the Silicon Age. Today, and likely for the foreseeable future, technological progress is increasingly defined by the development of nanomaterials [1] and smart materials [2]. The urgency of contemporary global challenges such as climate change demands, at least in part, innovative material solutions. A crucial aspect of this effort lies in the development of energy-efficient and renewable energy-harvesting technologies. An example of the latter are solar cells, which harness sunlight to generate electricity, whereas the former is well embodied by smart windows, which dynamically regulate heat and light transfer to improve energy efficiency in buildings. Additionally, a key sustainability goal is to manufacture widespread technological devices, such as displays or touchscreens for electronic devices, or transparent heaters for vehicles or medical applications, using less material, ideally from more abundant resources. A common requirement for all these applications is the need for transparent electrodes: materials that conduct electricity while *simultaneously* allowing light to pass through. This combination defines the class of Transparent Conducting Materials (TCMs). At first glance, this dual property may seem counter-intuitive, as electrical conductivity and optical transparency are typically found at opposite ends of the material spectrum. Metals, for instance, are excellent conductors but opaque to visible light, while transparent materials such as glass are usually electrical insulators. Yet, TCMs bridge this apparent contradiction, making them essential for applications such as the above-mentioned touchscreens, solar cells, or smart windows. Currently, the most widespread TCMs are Transparent Conducting Oxides (TCOs), the most used and researched of which is Indium Tin Oxide (ITO) due to its outstanding electro-optical properties [3]. However, ITO faces significant limitations. It relies on indium, a material classified by the European Commission as critical due to its scarcity [4]: it is a byproduct of zinc mining, and its supply cannot be easily scaled to meet increasing demand [5]. In addition, it lacks mechanical flexibility, making it unsuitable for emerging flexible electronics, and, more critically, making it prone to degradation due to unwanted mechanical bending that can occur for a variety of reasons (strain-inducing temperature gradient, transport, fabrication processes, etc.) [6, 7].

As a consequence of these drawbacks, extensive research has focused on identifying viable alternatives to ITO-based TCMs [8]. Several promising options have emerged over the years,

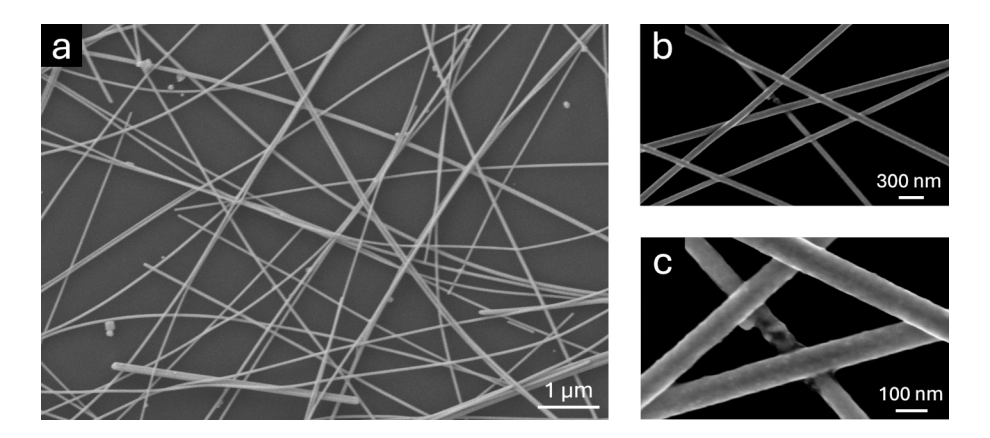


Figure 1: Scanning Electron Microscope (SEM) images of silver nanowire networks at varying magnifications. Image (a) highlights the high aspect ratio of the nanowires, which extend over several micrometers in length. Closer views in images (c) and (d) reveal their nanoscale diameters, typically in the range of tens of nanometers. These dimensions are characteristic of AgNWs used in transparent conducting materials, combining long-range connectivity with minimal optical obstruction. Numerous junctions and overlaps between nanowires are visible, eventually allowing the formation of a percolating network that enables electrical conductivity across the sample.

such as carbon nanotubes [9], graphene [10], conductive polymers [11], metallic grids [12], and networks of metallic nanowires [13–15]. Among these, silver nanowire (AgNW) networks have attracted particular attention. They offer electro-optical properties comparable to ITO [16] while overcoming its main drawbacks: they are highly flexible [17, 18], require significantly less material thanks to their nanostructured nature, and can be manufactured using cost-effective, scalable techniques such as roll-to-roll coating [19, 20]. In addition, they can easily be coated with protective oxides such as ZnO or SnO₂ to enhance their stability [21, 22]. It is also noteworthy that unlike ITO, AgNW networks have the ability to reduce the heat emission of a material [23, 24]. This property, known as low-emissivity in the infrared, paves the way to applications beyond electronics. For example, they can help regulate heat transfer through windows, making them excellent candidates for energy-saving smart windows in buildings—a direction we have explored in detail in some of our most recent work [25].

Silver nanowire networks belong to the family of transparent conducting materials, but they differ significantly in structure from traditional materials like ITO. As shown in Fig. 1, instead of forming a continuous film, they are made up of a random arrangement of high aspect-ratio silver wires, each typically tens of nanometers in diameter but stretching up to tens of micrometers in length [26]. The key to their optical transparency lies in their structure. Because the wires are spread out and do not completely cover the surface, there are empty spaces between them through which light can pass freely. It is the nanoscale equivalent to looking through a sparse net or tennis racket: if the threads are thin and far apart, you can see right through it.

While transparency in silver nanowire networks comes from the empty spaces between the

wires, electrical conductivity is all about the connections. Each individual nanowire is highly conducting—after all, they are made of silver, one of the best electrical conductors [27]. But for the entire network to conduct across a surface, the nanowires must touch and overlap, forming continuous pathways for current to flow. This can be pictured as a network of roads: it does not matter how smooth each road is; if they do not connect, you will never reach your destination. Similarly, in AgNW networks, the current travels by flowing from wire to wire through junctions scattered throughout the structure [28, 29]. Because the nanowires are randomly arranged, the resulting pathways form a complex web of series and parallel connections that make the overall electrical behavior quite intricate. Predicting how electrical current will flow through such a network, and thus determining its macroscopical conductance, is neither trivial nor straightforward since it depends not just on how many wires there are, but also and most importantly on the topology of the network [30]. However, being able to determine whether a network is electrically active, and understanding the link between its global and local properties, is of major importance when designing TCMs based on random NW networks [13, 31]. Furthermore, unraveling the stochastic and interdependent phenomena underlying this link allows for better control over the network's arising properties such as its electrical resistance, and required density for the design and fabrication of optimized and cost-efficient NW networks [32]. The domain within which this specific type of investigation is inscribed is called *percolation* theory.

2. Concepts of Percolation Theory

While the term *percolation* was familiarly coined to describe the flow of water through coffee powder, the scope of this theory extends much more widely and fundamentally [33]. Percolation theory offers a fundamental lens through which we can understand how connectivity emerges in disordered systems. Originally developed to describe how fluids flow through porous materials, its concepts have since found broad application across fields as diverse as epidemiology [34], materials science [35], and biology [36]. At its core, percolation theory deals with the probability that local connections—whether between pores, individuals, or structural elements—can form a continuous path spanning an entire system. A central insight, introduced by Broadbent and Hammersley in 1957, is that the ability for something to flow through a medium often depends more on the geometry and randomness of the *medium itself* than on the properties of the flowing agent [37]. This shifted the perspective through which such phenomena were studied from the behavior of the "fluid" (e.g., water, electricity, or information) to the structure of the system through which it moves.

To formalize this, Broadbent and Hammersley introduced the **bond percolation model**. In this model, the system is represented as a regular lattice of discrete *sites* (or *vertices*) connected by *bonds* (or *edges*), each of which has a probability p of being open (allowing connection) and a probability 1-p of being closed (blocking flow). If enough bonds are open, a spanning path emerges across the system. A classic example is water flowing through a porous rock: the open bonds represent channels between pores through which water can pass. This is illustrated in Fig. 2a,b. A related model, known as **site percolation**, instead considers randomness at the

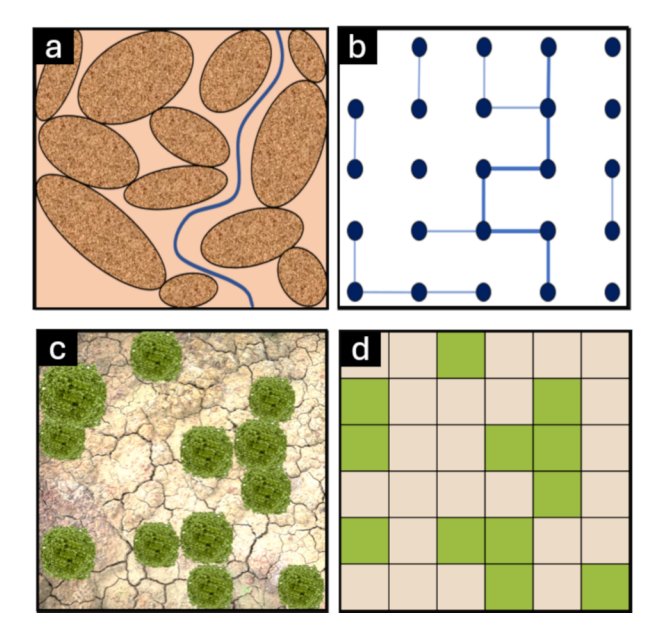


Figure 2: (*a*–*b*) Illustration of the bond percolation model applied to a porous material. (*a*) Schematic of a porous stone where open pores are connected via open or closed passages; a continuous path for water flow is shown in blue. (*b*) Corresponding bond percolation model on a square lattice: sites represent pores, and open passages are depicted as edges—light blue for general connections, dark blue for those forming the main flow path. Absence of an edge denotes a closed passage. (*c*–*d*) Site percolation model applied to forest fire propagation. (*c*) Schematic of a sparse forest. (*d*) Site percolation representation: light green cells indicate trees (open sites), brown cells indicate empty ground (closed sites). Fire can only spread through adjacent trees; in this example, no path connects the top to the bottom, meaning the fire cannot propagate through the entire forest.

level of the sites themselves. Each site is either open or closed with probability p or 1-p, respectively, and connectivity occurs only between adjacent open sites. This model is schematized in Fig. 2c,d. Both models raise the central question of percolation theory: given a certain probability p, what is the likelihood R(p) that a connected path exists across the system?

While these models are defined on regular grids, many real-world systems lack such orderly structure. This motivates the study of **continuum percolation**, in which elements are distributed randomly in continuous space. Unlike lattice-based models, where positions are fixed and periodic, continuum systems involve additional spatial disorder, introducing greater mathematical and computational complexity [38]. A particularly relevant—and convenient—example is the case of *metallic nanowire networks*, such as those made from silver nanowires deposited on insulating substrates. In this context, the nanowires act as the sites of the system, and electrical current flows when enough of them overlap to form connected pathways. In such networks, the key control parameter is the nanowire density n, typically defined as the number of wires per unit area. The percolation probability R(n) describes the likelihood that a conduc-

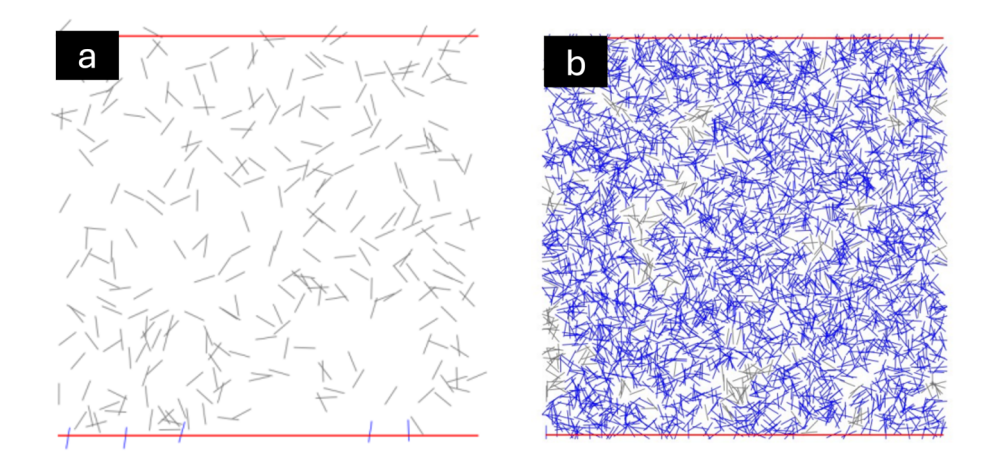


Figure 3: Schematic representation of (a) a non-percolating and (b) a percolating nanowire network. In (a), the nanowire density is too low to form sufficient overlaps, preventing the formation of a conductive path between the top and bottom electrodes (shown in red). Nanowires connected to the bottom electrode local clusters are highlighted in blue. In (b), the higher nanowire density results in the formation of a spanning cluster: a continuous network of interconnected wires that bridges the top and bottom electrodes. Nanowires not part of the spanning cluster are shown in gray.

tive path spans the entire system (from electrode to electrode) at a given density, as displayed in Fig. 3. As with classical percolation, a threshold density n_c exists: below this value, the network is almost certainly non-conductive, while above it, a percolating cluster forms with high probability. In an idealized, infinitely large system, the transition is abrupt:

$$R(n) = \begin{cases} 0 & \text{if } n < n_{\text{c}}, \\ 1 & \text{if } n \ge n_{\text{c}}. \end{cases}$$
 (1)

This discontinuous jump in R(n) arises from a well-known probabilistic principle called Kolmogorov's zero—one law [39], which ensures that in the infinite-size limit, the system either percolates with certainty or not at all: there is no in-between. In practice, however, all systems are finite. In such cases and as displayed in Fig. 4, the transition is smooth rather than abrupt, and the percolation probability follows a sigmoidal curve. The *steepness* of this curve increases with the system's size L_s , and the probability is therefore written more precisely as $R_{L_s}(n)$. To characterize the threshold in finite systems, Reynolds and Klein introduced the effective percolation density $n_{0.5}(L_s)$, defined as the density at which the system has a 50% chance of percolating [40]:

$$R_{L_{\rm s}}(n_{0.5}(L_{\rm s})) = \frac{1}{2}.$$
 (2)

This concept is widely used in numerical studies and experiments to estimate percolation thresholds of AgNW network samples. When the system is large enough to enter the so-called scaling regime, the threshold $n_{0.5}(L_s)$ becomes nearly size-independent, a property that reflects the scale

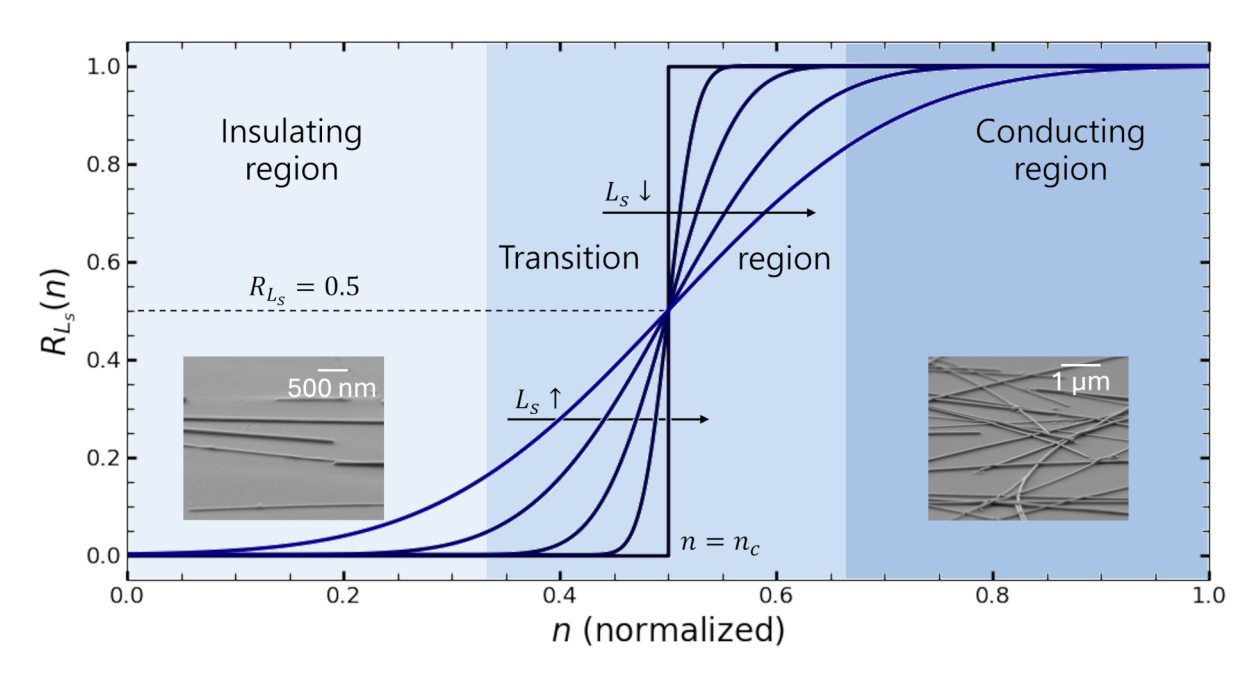


Figure 4: The evolution of the percolation probability $R_{L_s}(n)$ as a function of normalized nanowire density n. As the system size L_s increases, the transition from non-percolating to percolating becomes steeper, approaching a sharp step at the percolation threshold n_c in the limit of an infinitely large system. In the insulating regime (low n), the high sparsity of NWs prevents the formation of continuous conductive paths, and the network cannot percolate. In the transition region, where n is close to n_c , scaling laws of percolation apply: adding NWs increases the probability of forming new connections that allow current to flow across the system. In the conducting regime (high n), the network is already fully connected, and further increases in NW density have little impact on the overall conductance. Insets: SEM images showing a sparse NW network (*left*) and a relatively dense NW network (*right*).

invariance characteristic of continuous phase transitions [41]. At this point, patterns of connectivity become self-similar across scales, and the system's macroscopic behavior is governed by collective statistical rules rather than microscopic details [42].

For the specific case of two-dimensional networks of randomly oriented sticks (a reasonably accurate model for AgNW networks), pioneering Monte Carlo simulations by Pike and Seager (1971) provided the first estimates of the percolation threshold [43]:

$$n_{\rm c} = \frac{5.71 \pm 0.24}{l^2},\tag{3}$$

where l is the nanowire length. Later refinements by Li and Zhang led to a much more precise determination [44]:

$$n_{\rm c} = \frac{5.63726 \pm 0.00002}{l^2}.\tag{4}$$

This critical density serves as a valuable benchmark for designing nanowire networks optimized for minimal material usage while ensuring electrical connectivity. Understanding and accurately

modeling this threshold is essential for the rational design of efficient transparent conducting materials with low environmental impact. However, while informative, this expression alone is not sufficient for practical applications. To derive usable and predictive guidelines for real-world devices, one must examine deeper the theoretical framework of percolation, where more complex and application-relevant insights can be uncovered.

Another key outcome of percolation theory is the scaling relation between network conductivity and nanowires density:

$$\sigma \propto (n - n_{\rm c})^t,\tag{5}$$

where σ is the electrical conductivity, the tendency of a material system to conduct electricity, and t is called the apparent conductivity exponent. First identified by Kirkpatrick in 1973 [45], this equation is central to the study of networks consisting of nanowires, nanotubes, and other high aspect ratio (nano) structures [46]. As mentioned earlier, while the knowledge of n_c alone serves as a valuable tool to determine the minimum required amount of nanowires to achieve minimal conductivity, it is the detailed insights into network conductivity and topology that Eq. (5) brings that are of crucial importance when studying such complex networks. Furthermore, such understanding enables the estimation of a network's conductivity from fundamental parameters, guiding the optimization of material properties for specific applications. Understanding how physical and geometrical factors influence the variables in this equation is therefore crucial—not only for uncovering the fundamental physics of these materials—but also for designing high-performance conductive networks.

Percolation theory predicts a universal exponent $t = \mu$, with a theoretical value of $\mu = 1.3$ in two-dimensional (2D) settings [42]. For metallic nanowire networks, the system is generally considered 2D since the out-of-plane components contribute minimally to conduction [47]. The universal aspect of this law refers to the independence of t on the type of lattice considered, be it a discrete honey-comb or continuous random nanowire network. Near the percolation threshold $n_{\rm c}$, the system loses all memory of its microscopic structure. Instead, it starts to behave as a scale-invariant system: patterns repeat at different length scales, much like a fractal. At this point, the system undergoes a phase transition (from being non-conductive to conductive) and its collective properties, rather than individual details, start to govern its emerging macroscopic behavior. This is why different systems, even if their components or arrangements vary greatly, can exhibit the same scaling behavior when they are close to this critical point. The universal exponents that describe this behavior, like μ for the conductivity, are an elegant signature of that transition. They do not depend on the precise shape, size, or placement of the elements in the system, but only on very general features such as dimensionality (2D vs. 3D). While we will focus here on the exponent governing electrical conductivity, the one most important for practical applications of AgNW networks, it is noteworthy that percolation theory actually contains a whole set of such critical exponents, each describing how a different physical quantity (cluster size, correlation length, probability of forming a spanning cluster, etc.) behaves near the percolation threshold [48]. Together, these exponents provide a rich framework to understand the scaling laws that govern many disordered and complex systems in nature.

In our research group, we work at the intersection of theoretical percolation models and

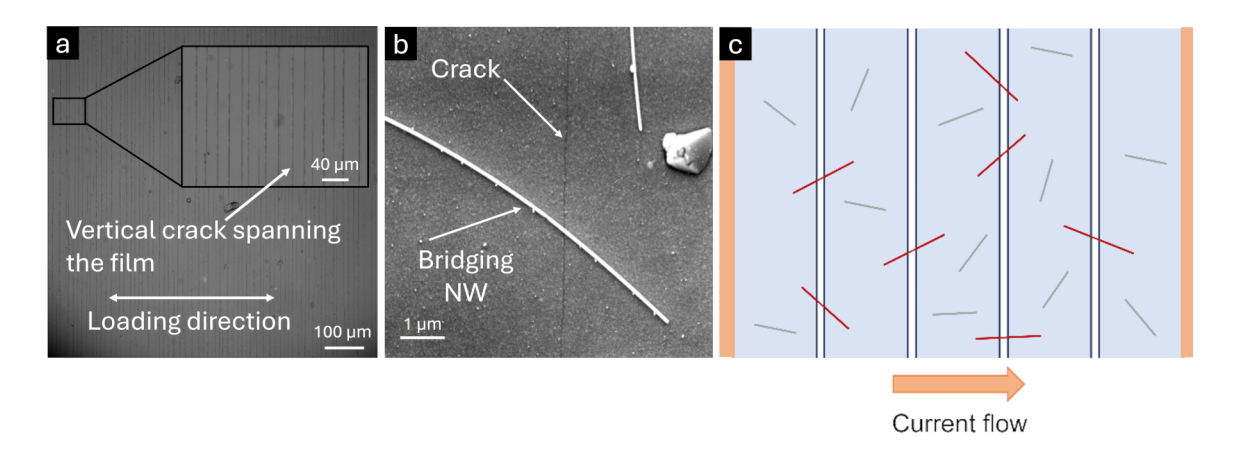


Figure 5: Illustrations of the hybrid material system. (a) SEM image of a fractured ITO thin film bent along the indicated direction. Inset: magnified view of parallel fractures. (b) A silver nanowire bridging a crack, reestablishing conduction across the gap. (c) Schematic of the system: electrodes (orange), bridging NWs (red), and non-participating NWs (light gray). Crack width is exaggerated for clarity. Percolation occurs when all cracks are spanned by nanowires. Reproduced from Ref. [49] with permission from the Royal Society of Chemistry.

real-world experimental systems. Our goal is to bridge the gap between abstract theory and practical application by exploring how the principles of percolation translate to the behavior of actual materials and devices. This involves tackling both the conceptual questions raised by percolation theory and the experimental challenges that arise when trying to apply it. In the next section, we present a selection of our contributions in this area.

3. On the Original Concept of Bridge Percolation

In recent work, we have presented the design of a new composite material which combines sparse metallic nanowire networks (i.e., with densities below the network critical density) and fractured conducting thin films on flexible insulating substrates (such as polymers) [49]. This concept takes inspiration from the well-characterized fracture behavior of ITO thin films when subjected to mechanical deformation on flexible substrates [50]. It is now well established that applying uni-axial stress to such brittle films leads to the formation of long, narrow (\approx 100 nm) cracks that break electrical continuity by isolating regions of the conductor [51–53]. Due to the crystalline nature of ITO, these cracks often appear as highly linear features, typically running in parallel and spanning the entire length of the film (Fig. 5a) perpendicularly to the applied stress direction [54]. This behavior is especially relevant in foldable electronics, where bending stress is commonly applied in a single direction, causing cracks to align accordingly.

To analyze conduction in such a system, we introduce the original concept of **bridge perco-lation**—a percolation process that occurs not through a fully insulating medium, but one where a partially conducting film is disrupted by non-conducting gaps. These gaps, corresponding to cracks in the film, can be spanned by randomly deposited NWs that restore electrical connectivity between the separated conducting regions (Fig. 5b,c). When enough cracks are bridged, a

continuous conducting path forms from one electrode to the other. Because most of the surface remains conducting, this mechanism is expected to require significantly fewer nanowires than traditional percolation networks.

One of the primary goals of this study is to quantify the critical NW density required to initiate bridge percolation for a given cracked substrate. This system offers an appealing opportunity: the ability to "repair" fractured conductive layers by overlaying them with sparse nanowire networks produced through cost-effective deposition techniques. This strategy could significantly improve the mechanical durability of devices relying on brittle transparent conductors like ITO. To model this system, we treat each NW as a potential bridge across a nonconductive gap, and seek to determine the minimum number required to form a spanning path. The percolation threshold thus depends on geometrical parameters such as crack density and nanowire dimensions. We also examine the evolution of electrical conductivity by adapting techniques previously developed for standard 2D NW networks, and compare our findings with classical percolation models.

Our derivation draws inspiration from a classic problem in probability theory known as *Buffon's needle problem*, posed in the 18th century and commonly stated as follows: "Suppose we have a floor made of parallel strips of wood, each the same width, and we drop a needle onto the floor. What is the probability that the needle will lie across a line between two strips?" [55] (Buffon himself actually formulated it in a slightly different way—see Refs. [56, p. 44] and [57, pp. 100–101].) Interestingly, the solution to this problem later led to an original manner of estimating the value of π [58]. While we omit the full derivation here (it is based on statistical and geometrical reasoning), we present the resulting expression, which gives the probability of percolation as a function of the areal mass density (*amd*). The *amd* is defined as the mass of nanowires per unit area, a more practically relevant quantity for the design and fabrication of AgNW-based devices but in essence strictly equivalent to the nanowire density n introduced before. The resulting expression is given by

$$R_{L_{\rm s}}(amd) = \left(1 - \left(1 - \frac{1}{L_{\rm s}}\right)^{\left(\frac{L_{\rm s}^2 \cdot amd}{m}\right)}\right)^{N_{\rm cr}},\tag{6}$$

where m is the mass of a single nanowire, L_s is the system size, and N_{cr} is the number of cracks. The function $R_{L_s}(amd)$ follows the sigmoidal trend typical of percolation transitions [42]. To better understand and analyze the influence of physical parameters on the percolation probability, it is better suited to study the evolution of amd_c as a function of the physical parameters of the system. By using the definition introduced in Eq. (2), we find:

$$amd_{c} = -\frac{m}{L_{s}} \cdot \frac{\ln\left(1 - 2^{-L_{cr}/L_{s}}\right)}{\bar{L}_{p}},\tag{7}$$

where m is the mass of an individual nanowire, L_s is the system's size, L_{cr} is the distance between adjacent fractures, and $\bar{L}_p = \frac{2 \times L_{NW}}{\pi}$ is the average projected length of the nanowires. The various geometrical features associated with the model are summarized in Fig. 6. Several

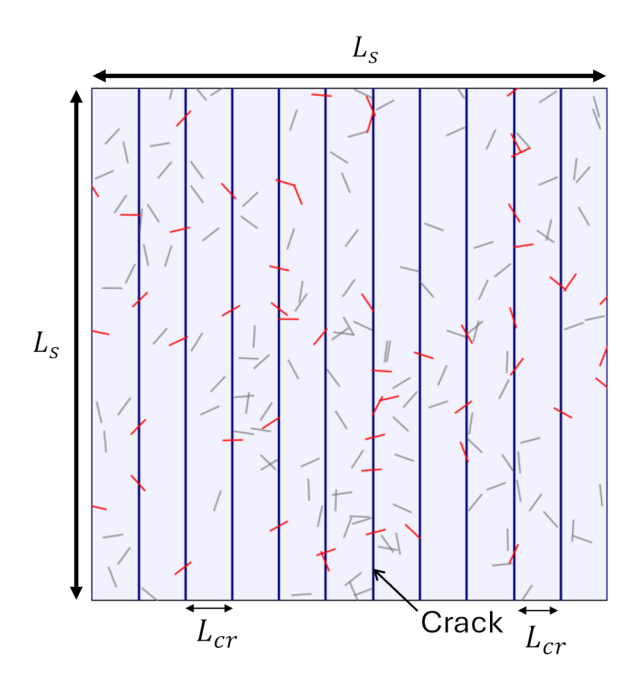


Figure 6: Schematic representation of the bridge percolation system used in simulations. The system consists of a square domain of size $L_{\rm s}$, containing regularly spaced vertical cracks separated by a distance $L_{\rm cr}$. Cracks are depicted in blue. Nanowires that successfully bridge the cracks and contribute to conduction are shown in red, while those that do not participate are shown in gray. For clarity, the illustration shows a magnified view of a small region within a much larger simulated system. Reproduced from Ref. [49] with permission from the Royal Society of Chemistry.

intuitive results emerge from this expression. First, shorter nanowires, as they span shorter distances, require a higher mass density to ensure percolation. Second, the logarithmic dependence on crack number is consistent with expected monotonic behavior in disordered systems [59]. Finally, and less intuitively, increasing the system size $L_{\rm s}$ leads to a *decrease* in the critical density: a notable difference from the scale-invariant behavior of classical percolation. This distinction arises from the system's inherent anisotropy. In the case of bridge percolation, electrical conduction can only occur across parallel cracks that span the height of the system. As the system grows, more cracks appear, and each crack must be bridged by at least one nanowire to ensure percolation. Since the number of cracks increases linearly with system size, the number of nanowires required to bridge them also increases linearly. However, because the system's area increases quadratically, the critical nanowire *density* decreases with system size. This breakdown of scale invariance is a direct result of the anisotropic geometry imposed by the aligned cracks, and it fundamentally distinguishes bridge percolation from classical models.

To test these purely theoretical models, which are notably free of any fitting parameter and designed to make quantitative, predictive claims, we turned to Monte Carlo simulations of the system. In simple terms, this computational method involves repeatedly simulating random versions of the network, to statistically understand how often it becomes conductive under certain

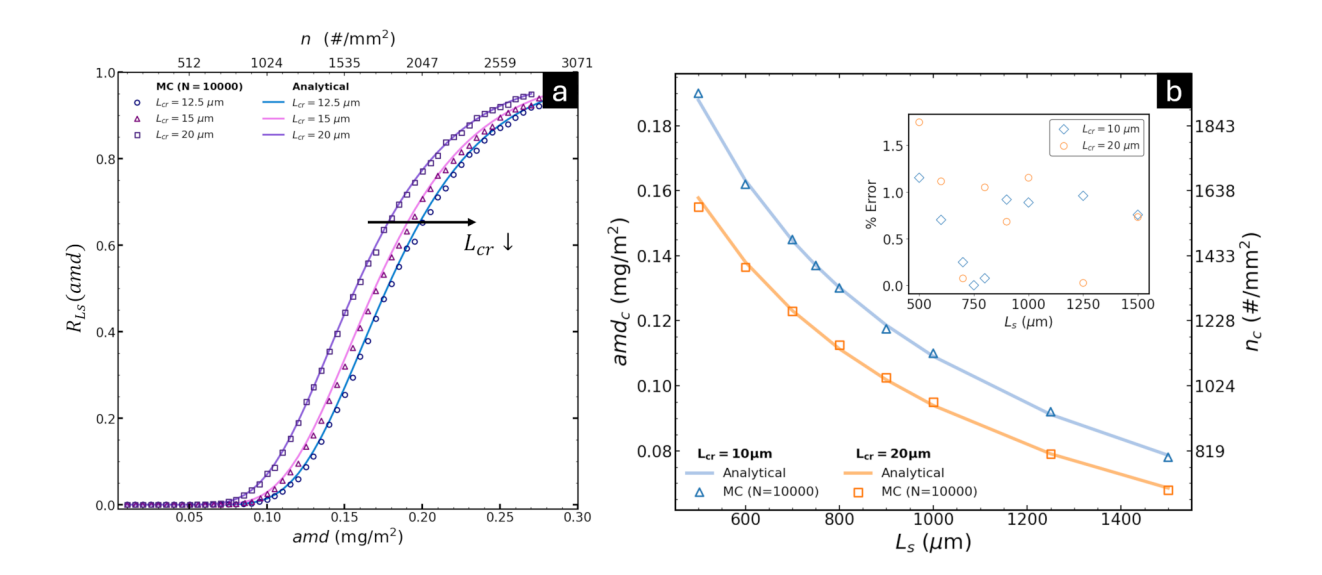


Figure 7: (a) Percolation probability as a function of the areal mass density (bottom x-axis) and nanowire number density (top x-axis) for three different crack spacings $L_{\rm cr}$. Solid lines correspond to the analytical predictions from Eq. (6), while the dots represent the results of Monte Carlo simulations, with N=10,000 trials per data point. (b) Evolution of the critical areal mass density (left axis) and critical nanowire density (right axis) as a function of the system size $L_{\rm s}$, shown for two values of crack spacing $L_{\rm cr}$. The solid curves represent the analytical model described by Eq. (7), and the dots indicate simulation results, also obtained with N=10,000 realizations per point. In both panels, simulations were performed on a 500 μm × 500 μm substrate using nanowires 7 μm in length and 50 nm in diameter. Reproduced from Ref. [49] with permission from the Royal Society of Chemistry.

conditions. In our case, each simulation consists in randomly placing silver nanowires into a virtual square area that mimics a fractured substrate. The key question we ask is: how many nanowires are needed for a continuous conducting path to appear across the system? That point marks the percolation threshold. By running this simulation 100,000 times, we can determine the critical nanowire density with high precision. This large number of repetitions helps us account for the inherent randomness in the system and extract robust, statistically meaningful results. Because of the sheer volume and size of these simulations—necessary to properly capture the inherently stochastic behavior of the network—we relied on the CECI supercomputing infrastructure to run our code, which provided the computational power needed to perform these calculations efficiently [60].

The comparison between our analytical model and Monte Carlo (MC) simulations, shown in Fig. 7, demonstrates excellent quantitative agreement, with discrepancies remaining below 2%. In these simulations, the crack spacing $L_{\rm cr}$ was held constant at values representative of those commonly observed in experimental conditions. A particularly striking result is that the critical areal mass density (amd_c) required for bridge percolation is significantly lower than the

threshold typically associated with classical 2D nanowire networks. Experimental studies have reported percolation thresholds for traditional systems ranging from 1 to 25 mg/m², depending on nanowire geometry. In contrast, the values predicted by our model for bridge percolation are around 0.1 mg/m², as highlighted in Fig. 7b. Additionally, Fig. 7b confirms the expected trend: the critical *amd* decreases with increasing system size. These findings validate the predictive accuracy of our theoretical framework and, more broadly, emphasize the potential of hybrid systems to achieve percolation with significantly less material than conventional approaches.

However and as mentioned earlier, reaching the percolation threshold is not sufficient for practical applications, particularly in the context of transparent conducting materials where low electrical resistance is a critical requirement. At the onset of percolation, a single conductive path spans the system, but its resistance remains too high for real-world applications. Improving conductivity requires increasing the nanowire density beyond the percolation threshold to enable multiple parallel paths and reduce overall resistance. To investigate this aspect, we developed an electrical model for the hybrid system that accounts for its key physical and statistical features. The total resistance of the network is determined by three main contributions: the resistance of the conductive thin film sections, the resistance of the bridging nanowires, and the residual resistance associated with the cracks themselves. Although cracks interrupt the continuity of the film, there remains a thin ductile layer of ITO at the base, which retains finite conductivity. This partial conduction is incorporated into the model by defining an initial resistance R_0 , representing the resistance of the fractured thin film (assumed here to be ITO, though the approach is applicable to other conductive materials with similar failure mechanisms). We translate the physical structure of the system into an equivalent electrical circuit model, where resistors connect voltage nodes, and each resistance value depends on both material properties and geometry. To solve this circuit, we implemented a numerical method based on the Modified Nodal Analysis (MNA), and ran simulations using high-performance computing resources provided by the CECI supercomputers. This allowed us to study how different physical parameters such as nanowire density, wire length, crack spacing, and system size, influence the overall electrical resistance of the composite.

The results presented in Fig. 8 illustrate the evolution of the electrical properties of the hybrid system as a function of the areal mass density (amd) of deposited nanowires. Figure 8a shows the sheet conductance plotted as a function of the amd. The data follow a clear power-law behavior, consistent with the form predicted by percolation theory for systems well above the critical threshold. Specifically, for $n > 6n_c$, we observe that the conductivity scales according to the relationship described in Eq. (5). A least-squares fit yields a critical exponent $t = 1.77 \pm 0.02$, which falls within the range of values typically associated with classical 2D percolation systems. This result strongly supports the idea that bridge percolation belongs to the same universality class as standard percolation mechanisms, while exhibiting distinct features due to its directional geometry and hybrid nature. Figure 8b presents the same data from a different perspective by plotting the sheet resistance as a function of amd. This representation emphasizes the substantial drop in resistance that accompanies increased nanowire coverage. Together, Figs. 8(a) and 8(b) offer complementary views of the same phenomenon: the former highlights the scaling laws governing conductivity, whereas the latter stresses the practical

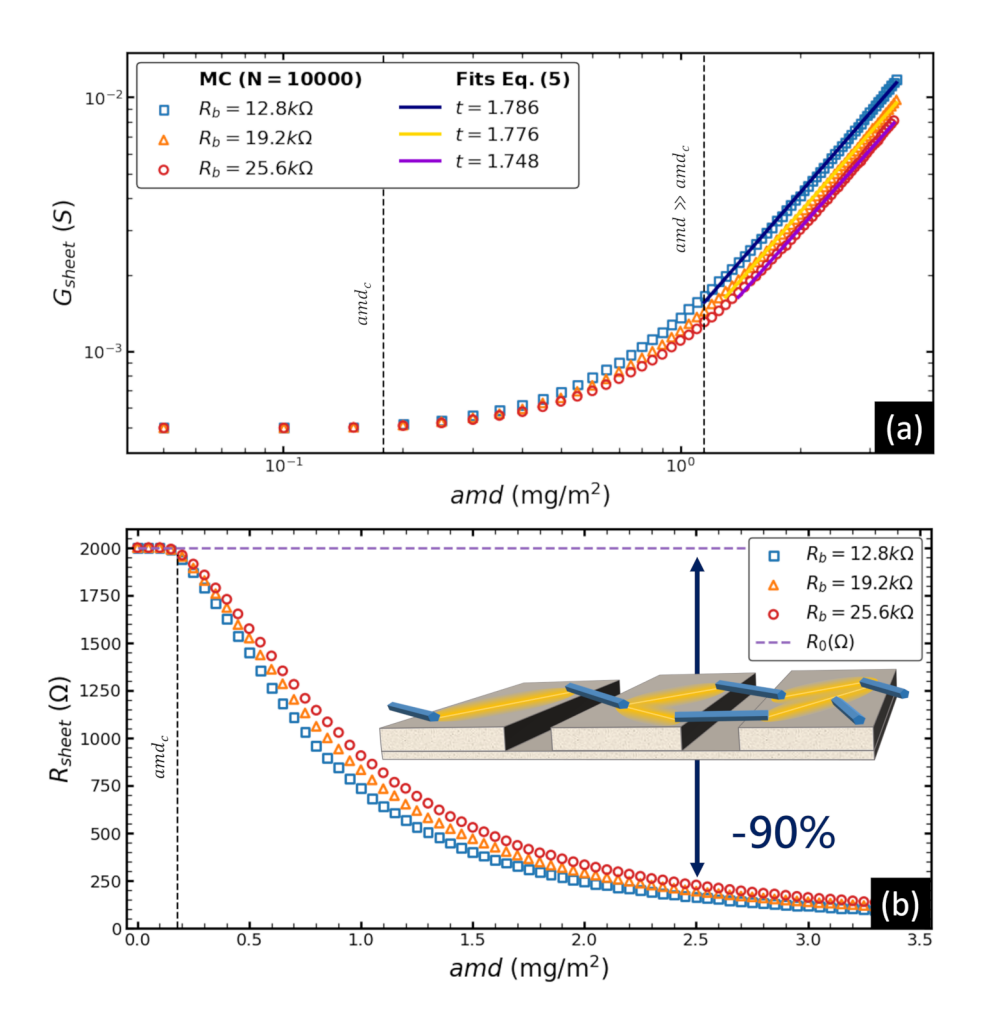


Figure 8: Monte Carlo simulation results showing the evolution of the conductance G_{sheet} and resistance R_{sheet} of the hybrid system as a function of the areal mass density (amd) for different values of the bridge resistance $R_{\rm b}$, corresponding to interfacial resistivities $\rho_{\rm b}$ of 1.6, 2.4, and $3.2 \,\Omega \cdot \text{cm}^2$. The critical *amd* associated with the system's geometry is indicated in each case. (a) Log-log plot of the sheet conductance, illustrating the power-law scaling behavior of the hybrid system at high nanowire densities, as described by Eq. (5). The slope corresponds to the universal conductivity exponent t introduced in Eq. (5), characteristic of percolating systems. (b) Sheet resistance as a function of amd, showing a rapid decrease in resistance beyond the percolation threshold. The inset provides a schematic representation of current flow through the hybrid system, with nanowires bridging the cracks in the fractured ITO layer. A blue line highlights the drop in resistance by 90% relative to its initial value, achieved with the deposition of just 3.5 mg/m² of Ag-NWs. The schematic inset also helps visualize how bridging nanowires reconnect isolated regions of the substrate, enabling effective conduction across the device. Reproduced from Ref. [49] with permission from the Royal Society of Chemistry.

outcome, namely, the significant improvement in electrical performance.

From a practical standpoint, we observe that depositing as little as 3.5 mg/m² of silver nanowires leads to a resistance reduction of up to 90%. This value is remarkably low when compared to conventional AgNW networks, which typically require areal mass densities in the range of 100–130 mg/m² to achieve similar electrical activation. In other words, bridge percolation enables efficient electrical conduction using over 35 times less silver. This material efficiency is particularly valuable in the context of scalable and sustainable manufacturing. It reduces production costs and minimizes the use of critical resources, which is increasingly important for environmentally friendly electronics and large-area applications such as flexible displays and solar cells.

4. Conclusions and Perspectives

In this work, we offer an angle to address the urgent need for sustainable and efficient transparent conducting materials by exploring silver nanowire networks as a promising alternative to conventional ITO. Thanks to their excellent electrical performance, mechanical flexibility, and low material requirements, AgNWs offer a compelling solution for applications such as photovoltaics, smart windows, and flexible electronics. To understand how such disordered nanoscale systems give rise to macroscopic conductivity, we introduced and explained the core concepts of percolation theory, providing a clear theoretical foundation to interpret the behavior of nanowire networks. Building on this, we developed the original concept of bridge percolation, a novel conduction mechanism that emerges when sparse nanowires are deposited on fractured conductive films, reconnecting isolated regions by bridging cracks. Through analytical modeling and extensive Monte Carlo simulations, we demonstrated that this hybrid architecture can achieve percolation using over 35 times less material than conventional AgNW networks. Beyond its practical relevance, bridge percolation also departs from the scale-invariant behavior of classical percolation due to its directional nature. Our results, at the intersection of mathematical theory and materials science, bridge fundamental insights with practical innovation, pointing toward lighter, cheaper, and more resilient TCMs for the next generation of energy-relevant technologies.

Looking ahead, we are extending this work to address one of the key remaining challenges facing silver nanowire networks: their thermal instability. At temperatures exceeding 250 °C, AgNWs undergo an irreversible morphological transition to a degraded state, which heavily compromises their conductivity by severely reducing the amount of intersections between nanowires and limits their use in high-temperature applications such as transparent heaters for medical or industrial devices. This behavior is often interpreted through the lens of the Plateau–Rayleigh instability, a classical fluid mechanics phenomenon originally described by Joseph Plateau (who, fittingly, earned his PhD at the University of Liège in 1837) [61]. Nearly two centuries later, we aim to continue in his footsteps, using modern tools in computation and nanoscale characterization to shed new light on the mechanisms that govern nanowire degradation [62]. By deepening our understanding of these phenomena, we hope to advance the design

of next-generation TCMs that are not only more sustainable, but also more stable and versatile under demanding operating conditions.

Acknowledgments

The author is indebted to Prof. N. D. Nguyen for his support, help and guidance. The author gratefully acknowledges the financial support by the European Commission via the M-ERA.NET program (INSTEAD project). Computational resources have been provided by the *Consortium des Équipements de Calcul Intensif* (CECI), funded by the Fonds de la Recherche Scientifique – FNRS (F.R.S.–FNRS) under Grant No. 2.5020.11 and by the Walloon Region. Financial support from F.R.S.–FNRS is gratefully acknowledged via the CDR project J.0124.19 and the PINT-MULTI project R.8012.20.

Further Information

Author's ORCID identifier

0000-0001-5037-9053 (Amaury BARET)

Conflicts of interest

The author declares that there is no conflict of interest.

References

- [1] Husain, M. and Khan, Z. H. (editors) (2016) *Advances in Nanomaterials*, *Advanced Structured Materials*, volume 79. Springer India, New Delhi (IN). https://doi.org/10.1007/978-81-322-2668-0.
- [2] Harvey, J. A. (2006) Smart materials. In *Mechanical Engineers' Handbook: Materials and Mechanical Design*, edited by Kutz, M., chapter 11, pages 418–432. John Wiley & Sons, Hoboken (US-NJ), 3. edition. https://doi.org/10.1002/0471777447.ch11.
- [3] Minami, T. (2005) Transparent conducting oxide semiconductors for transparent electrodes. *Semiconductor Science and Technology*, **20**(4), S35–S44. https://doi.org/10.1088/0268-1242/20/4/004.
- [4] Blengini, G. A., Latunussa, C. E. L., Eynard, U., Torres de Matos, C., Wittmer, D., Georgitzikis, K., Pavel, C., Carrara, S., Mancini, L., Unguru, M., Blagoeva, D., Mathieux, F., and Pennington, D. (2020) *Study on the EU's List of Critical Raw Materials* (2020): *Final Report*. Publications Office of the European Union, Luxembourg. https://doi.org/10.2873/11619.

- [5] Lokanc, M., Eggert, R., and Redlinger, M. (2015) *The Availability of Indium: The Present, Medium Term, and Long Term.* Technical Report NREL/SR–6A20-62409, National Renewable Energy Laboratory, Golden (US-CO). https://doi.org/10.2172/1327212.
- [6] Jung, H. S., Eun, K., Kim, Y. T., Lee, E. K., and Choa, S.-H. (2017) Experimental and numerical investigation of flexibility of ITO electrode for application in flexible electronic devices. *Microsystem Technologies*, 23(6), 1961–1970. https://doi.org/10.1007/s00542-016-2959-3.
- [7] Park, J.-W., Kim, G., Lee, S.-H., Kim, E.-H., and Lee, G.-H. (2010) The effect of film microstructures on cracking of transparent conductive oxide (TCO) coatings on polymer substrates. *Surface and Coatings Technology*, **205**(3), 915–921. https://doi.org/10.1016/j. surfcoat.2010.08.055.
- [8] Nguyen, V. H., Papanastasiou, D. T., Resende, J., Bardet, L., Sannicolo, T., Jiménez, C., Muñoz-Rojas, D., Nguyen, N. D., and Bellet, D. (2022) Advances in flexible metallic transparent electrodes. *Small*, 18(19), 2106006. https://doi.org/10.1002/smll.202106006.
- [9] Blackburn, J. L., Barnes, T. M., Beard, M. C., Kim, Y.-H., Tenent, R. C., McDonald, T. J., To, B., Coutts, T. J., and Heben, M. J. (2008) Transparent conductive single-walled carbon nanotube networks with precisely tunable ratios of semiconducting and metallic nanotubes. *ACS Nano*, **2**(6), 1266–1274. https://doi.org/10.1021/nn800200d.
- [10] Hecht, D. S., Hu, L., and Irvin, G. (2011) Emerging transparent electrodes based on thin films of carbon nanotubes, graphene, and metallic nanostructures. *Advanced Materials*, **23**(13), 1482–1513. https://doi.org/10.1002/adma.201003188.
- [11] K, N. and Rout, C. S. (2021) Conducting polymers: A comprehensive review on recent advances in synthesis, properties and applications. *RSC Advances*, **11**(10), 5659–5697. https://doi.org/10.1039/d0ra07800j.
- [12] van de Groep, J., Spinelli, P., and Polman, A. (2012) Transparent conducting silver nanowire networks. *Nano Letters*, **12**(6), 3138–3144. https://doi.org/10.1021/nl301045a.
- [13] Sannicolo, T., Lagrange, M., Cabos, A., Celle, C., Simonato, J.-P., and Bellet, D. (2016) Metallic nanowire-based transparent electrodes for next generation flexible devices: a review. *Small*, **12**(44), 6052–6075. https://doi.org/10.1002/smll.201602581.
- [14] Ye, S., Rathmell, A. R., Chen, Z., Stewart, I. E., and Wiley, B. J. (2014) Metal nanowire networks: The next generation of transparent conductors. *Advanced Materials*, **26**(39), 6670–6687. https://doi.org/10.1002/adma.201402710.
- [15] Bellet, D., Lagrange, M., Sannicolo, T., Aghazadehchors, S., Nguyen, V., Langley, D., Muñoz-Rojas, D., Jiménez, C., Bréchet, Y., and Nguyen, N. (2017) Transparent electrodes based on silver nanowire networks: From physical considerations towards device integration. *Materials*, 10(6), 570. https://doi.org/10.3390/ma10060570.

- [16] Lagrange, M., Langley, D. P., Giusti, G., Jiménez, C., Bréchet, Y., and Bellet, D. (2015) Optimization of silver nanowire-based transparent electrodes: Effects of density, size and thermal annealing. *Nanoscale*, **7**(41), 17410–17423. https://doi.org/10.1039/c5nr04084a.
- [17] Sekkat, A., Sanchez-Velasquez, C., Bardet, L., Weber, M., Jiménez, C., Bellet, D., Muñoz-Rojas, D., and Nguyen, V. H. (2024) Towards enhanced transparent conductive nanocomposites based on metallic nanowire networks coated with metal oxides: a brief review. *Journal of Materials Chemistry A*, 12(38), 25 600–25 621. https://doi.org/10.1039/d4ta05370b.
- [18] Azani, M.-R., Hassanpour, A., and Torres, T. (2020) Benefits, problems, and solutions of silver nanowire transparent conductive electrodes in Indium Tin Oxide (ITO)-free flexible solar cells. *Advanced Energy Materials*, **10**(48), 2002536. https://doi.org/10.1002/aenm. 202002536.
- [19] Crêpellière, J., Menguelti, K., Wack, S., Bouton, O., Gérard, M., Popa, P. L., Pistillo, B. R., Leturcq, R., and Michel, M. (2021) Spray deposition of silver nanowires on large area substrates for transparent electrodes. *ACS Applied Nano Materials*, **4**(2), 1126–1135. https://doi.org/10.1021/acsanm.0c02763.
- [20] Deng, B., Hsu, P.-C., Chen, G., Chandrashekar, B. N., Liao, L., Ayitimuda, Z., Wu, J., Guo, Y., Lin, L., Zhou, Y., Aisijiang, M., Xie, Q., Cui, Y., Liu, Z., and Peng, H. (2015) Roll-to-roll encapsulation of metal nanowires between graphene and plastic substrate for high-performance flexible transparent electrodes. *Nano Letters*, 15(6), 4206–4213. https://doi.org/10.1021/acs.nanolett.5b01531.
- [21] Khan, A., Nguyen, V. H., Muñoz-Rojas, D., Aghazadehchors, S., Jiménez, C., Nguyen, N. D., and Bellet, D. (2018) Stability enhancement of silver nanowire networks with conformal ZnO coatings deposited by atmospheric pressure spatial atomic layer deposition. *ACS Applied Materials & Interfaces*, **10**(22), 19 208–19 217. https://doi.org/10.1021/acsami.8b03079.
- [22] Bardet, L., Akbari, M., Crivello, C., Rapenne, L., Weber, M., Nguyen, V. H., Jiménez, C., Muñoz-Rojas, D., Denneulin, A., and Bellet, D. (2023) SnO₂-coated silver nanowire networks as a physical model describing their reversible domain under electrical stress for stable transparent electrode applications. ACS Applied Nano Materials, 6(16), 15 234–15 246. https://doi.org/10.1021/acsanm.3c03008.
- [23] Bobinger, M., Angeli, D., Colasanti, S., La Torraca, P., Larcher, L., and Lugli, P. (2017) Infrared, transient thermal, and electrical properties of silver nanowire thin films for transparent heaters and energy-efficient coatings. *physica status solidi* (*a*), **214**(1), 1600466. https://doi.org/10.1002/pssa.201600466.
- [24] Larciprete, M. C., Albertoni, A., Belardini, A., Leahu, G., Li Voti, R., Mura, F., Sibilia, C., Nefedov, I., Anoshkin, I. V., Kauppinen, E. I., and Nasibulin, A. G. (2012) Infrared

- properties of randomly oriented silver nanowires. *Journal of Applied Physics*, **112**(8), 083503. https://doi.org/10.1063/1.4759374.
- [25] Baret, A., Khan, A., Rougier, A., Bellet, D., and Nguyen, N. D. (2025) Low-emissivity fine-tuning of efficient VO₂-based thermochromic stacks with silver nanowire networks. *RSC Applied Interfaces*, **2**(1), 94–103. https://doi.org/10.1039/D4LF00234B.
- [26] Bergin, S. M., Chen, Y.-H., Rathmell, A. R., Charbonneau, P., Li, Z.-Y., and Wiley, B. J. (2012) The effect of nanowire length and diameter on the properties of transparent, conducting nanowire films. *Nanoscale*, **4**(6), 1996–2004. https://doi.org/10.1039/C2NR30126A.
- [27] Matula, R. A. (1979) Electrical resistivity of copper, gold, palladium, and silver. *Journal of Physical and Chemical Reference Data*, **8**(4), 1147–1298. https://doi.org/10.1063/1. 555614.
- [28] Gomes da Rocha, C., Manning, H. G., O'Callaghan, C., Ritter, C., Bellew, A. T., Boland, J. J., and Ferreira, M. S. (2015) Ultimate conductivity performance in metallic nanowire networks. *Nanoscale*, **7**(30), 13 011–13 016. https://doi.org/10.1039/c5nr03905c.
- [29] Bellew, A. T., Manning, H. G., Gomes da Rocha, C., Ferreira, M. S., and Boland, J. J. (2015) Resistance of single Ag nanowire junctions and their role in the conductivity of nanowire networks. *ACS Nano*, **9**(11), 11422–11429. https://doi.org/10.1021/acsnano. 5b05469.
- [30] Balberg, I. (2020) The physical fundamentals of the electrical conductivity in nanotube-based composites. *Journal of Applied Physics*, **128**(20), 204304. https://doi.org/10.1063/5.0031257.
- [31] De, S. and Coleman, J. N. (2011) The effects of percolation in nanostructured transparent conductors. *MRS Bulletin*, **36**(10), 774–781. https://doi.org/10.1557/mrs.2011.236.
- [32] Langley, D. (2014) Silver Nanowire Networks: Effects of Percolation and Thermal Annealing on Physical Properties. Ph.D. thesis, Université de Grenoble and Université de Liège. https://hdl.handle.net/2268/177659.
- [33] Stauffer, D. (1979) Scaling theory of percolation clusters. *Physics Reports*, **54**(1), 1–74. https://doi.org/10.1016/0370-1573(79)90060-7.
- [34] Mello, I. F., Squillante, L., Gomes, G. O., Seridonio, A. C., and de Souza, M. (2021) Epidemics, the Ising-model and percolation theory: A comprehensive review focused on Covid-19. *Physica A: Statistical Mechanics and its Applications*, **573**, 125963. https://doi.org/10.1016/j.physa.2021.125963.
- [35] Bishop, A. R. (1973) Percolation theory and the Ising model. *Journal of Physics C: Solid State Physics*, **6**(13), 2089–2093. https://doi.org/10.1088/0022-3719/6/13/009.

- [36] Brunk, N. E. and Twarock, R. (2021) Percolation theory reveals biophysical properties of virus-like particles. *ACS Nano*, **15**(8), 12 988–12 995. https://doi.org/10.1021/acsnano. 1c01882.
- [37] Broadbent, S. R. and Hammersley, J. M. (1957) Percolation processes: I. Crystals and mazes. *Mathematical Proceedings of the Cambridge Philosophical Society*, **53**(3), 629–641. https://doi.org/10.1017/S0305004100032680.
- [38] Balberg, I. (2020) Principles of the theory of continuum percolation. In *Encyclopedia of Complexity and Systems Science*, edited by Meyers, R. A., pages 1–61. Springer, Berlin, Heidelberg (DE). https://doi.org/10.1007/978-3-642-27737-5_95-4.
- [39] Kherani, A. and Bagchi, A. (2007) Lecture 1: Overview of percolation and foundational results from probability theory. https://www.cse.iitd.ac.in/~bagchi/courses/CSL866_07-08/. Lecture notes for course CSL866: Percolation and Random Graphs, Indian Institute of Technology Delhi. Last access: 6 November 2025.
- [40] Reynolds, P. J., Stanley, H. E., and Klein, W. (1978) Percolation by position-space renormalisation group with large cells. *Journal of Physics A: Mathematical and General*, **11**(8), L199–L207. https://doi.org/10.1088/0305-4470/11/8/006.
- [41] Stauffer, D. (2009) Phase transitions on fractals and networks. In *Encyclopedia of Complexity and Systems Science*, edited by Meyers, R. A., pages 6783–6789. Springer, New York (US-NY). https://doi.org/10.1007/978-0-387-30440-3_406.
- [42] Stauffer, D. and Aharony, A. (1994) *Introduction to Percolation Theory*. CRC Press, 2. rev. edition.
- [43] Pike, G. E. and Seager, C. H. (1974) Percolation and conductivity: A computer study. I. *Physical Review B*, **10**(4), 1421–1434. https://doi.org/10.1103/PhysRevB.10.1421.
- [44] Li, J. and Zhang, S.-L. (2009) Finite-size scaling in stick percolation. *Physical Review E*, **80**(4), 040104. https://doi.org/10.1103/PhysRevE.80.040104.
- [45] Kirkpatrick, S. (1973) Percolation and conduction. *Reviews of Modern Physics*, **45**(4), 574–588. https://doi.org/10.1103/RevModPhys.45.574.
- [46] Bauhofer, W. and Kovacs, J. Z. (2009) A review and analysis of electrical percolation in carbon nanotube polymer composites. *Composites Science and Technology*, **69**(10), 1486–1498. https://doi.org/10.1016/j.compscitech.2008.06.018.
- [47] Mutiso, R. M. and Winey, K. I. (2013) Electrical percolation in quasi–two-dimensional metal nanowire networks for transparent conductors. *Physical Review E*, **88**(3), 032134. https://doi.org/10.1103/PhysRevE.88.032134.
- [48] Álvarez Álvarez, A., Balberg, I., and Fernández-Álvarez, J. P. (2021) Invariant percolation properties in some continuum systems. *Physical Review B*, **104**(18), 184205. https://doi.org/10.1103/PhysRevB.104.184205.

- [49] Baret, A., Bardet, L., Oser, D., Langley, D. P., Balty, F., Bellet, D., and Nguyen, N. D. (2024) Bridge percolation: electrical connectivity of discontinued conducting slabs by metallic nanowires. *Nanoscale*, **16**(17), 8361–8368. https://doi.org/10.1039/D3NR05850F.
- [50] Lee, S. (2019) *Mechanical Properties of Metal Based Flexible Transparent Conductive Electrode: From Fracture Mechanics Perspective*. Ph.D. thesis, University of Michigan. https://hdl.handle.net/2027.42/149813.
- [51] Chen, Z., Cotterell, B., and Wang, W. (2002) The fracture of brittle thin films on compliant substrates in flexible displays. *Engineering Fracture Mechanics*, **69**(5), 597–603. https://doi.org/10.1016/S0013-7944(01)00104-7.
- [52] Zhinong, Y., Longfeng, X., Wei, X., and Huaqing, W. (2007) The bending properties of flexible ITO films. In 2007 Asia Optical Fiber Communication and Optoelectronics Conference, pages 148–150. IEEE. https://doi.org/10.1109/AOE.2007.4410733.
- [53] Vlassak, J. J. (2003) Channel cracking in thin films on substrates of finite thickness. *International Journal of Fracture*, **119/120**, 299–323. https://doi.org/10.1023/A: 1024962825938.
- [54] Leterrier, Y., Médico, L., Demarco, F., Månson, J.-A. E., Betz, U., Escolà, M. F., Kharrazi Olsson, M., and Atamny, F. (2004) Mechanical integrity of transparent conductive oxide films for flexible polymer-based displays. *Thin Solid Films*, **460**(1-2), 156–166. https://doi.org/10.1016/j.tsf.2004.01.052.
- [55] Buffon's needle problem. Wikipedia [en ligne]. https://en.wikipedia.org/wiki/Buffon% 27s_needle_problem. Version of 2 October 2025; last access: 6 November 2025.
- [56] Académie royale des sciences (1735) Géométrie. *Histoire de l'Académie royale des sciences. Année M.DCCXXXV [1733]*, pages 43–45. https://gallica.bnf.fr/ark:/12148/bpt6k3530m. Last access: 6 November 2025.
- [57] Comte de Buffon (1777) Essais d'arithmétique morale. In *Histoire naturelle, générale et particulière: Supplément*, volume 4, pages 46–123. Imprimerie Nationale, Paris (FR). https://books.google.be/books?id=AjhYD1vsVAIC. Last access: 6 November 2025.
- [58] Uspensky, J. V. (1937) *Introduction To Mathematical Probability*. McGraw-Hill Book Company, New York (US-NY) and London (UK).
- [59] de Gennes, P. G. and Witten, T. A. (1980) Scaling concepts in polymer physics. *Physics Today*, **33**(6), 51–54. https://doi.org/10.1063/1.2914118.
- [60] CECI. https://www.ceci-hpc.be/.
- [61] Renotte, Y. (2024). Deux «savants contemporains» «deux destins» qui se sont «croisés» à l'Université de Liège ... mais ne se sont peut-être jamais rencontrés!

- Michel Gloesener (1794–1876) et Joseph Plateau (1801–1883). https://hdl.handle.net/2268/319323.
- [62] Balty, F., Baret, A., Silhanek, A., and Nguyen, N. D. (2024) Insight into the morphological instability of metallic nanowires under thermal stress. *Journal of Colloid and Interface Science*, **673**, 574–582. https://doi.org/10.1016/j.jcis.2024.06.074.